



NOTE

Pathology

Pathologic characterization of *Felis catus* papillomavirus type 5 (FcaPV-5)-associated viral plaques and Bowenoid *in situ* carcinoma in a Domestic Shorthair cat

Mun Keong KOK¹#, Nanako YAMASHITA-KAWANISHI²#, James. K. CHAMBERS¹*, Makoto HARITANI³, Takahiro USHIGUSA⁴, Takeshi HAGA², Hiroyuki NAKAYAMA¹ and Kazuyuki UCHIDA¹

¹Laboratory of Veterinary Pathology, Graduate School of Agricultural and Life Sciences, The University of Tokyo, 1-1-1 Yayoi, Bunkyo-ku, Tokyo 113-8657, Japan

²Laboratory of Infection Control and Disease Prevention, Graduate School of Agricultural and Life Sciences, The University of Tokyo, 1-1-1 Yayoi, Bunkyo-ku, Tokyo 113-8657, Japan

³Research Centre for Food Safety, Graduate School of Agricultural and Life Sciences, The University of Tokyo, 1-1-1 Yayoi, Bunkyo-ku, Tokyo 113-8657, Japan

⁴Kannai Animal Clinic, 6-3 Yoshida-cho, Naka-ku, Yokohama, Kanagawa 231-0041, Japan

ABSTRACT. The present paper describes *Felis catus* papillomavirus (FcaPV) type 5-associated cutaneous mass in a Domestic Shorthair cat. Histological examination revealed multicentric epidermal acanthosis with papillomavirus-associated cytopathic changes, which progressed to a tumor lobule with intact basement membrane. An association between FcaPV-5 and the cutaneous lesions was confirmed by detection of virus antigen and genes using immunohistochemistry, polymerase chain reaction (PCR), sequencing analysis, and *in situ* hybridization. Based on these findings, the lesions were diagnosed as FcaPV-5-associated viral plaques and Bowenoid *in situ* carcinoma (BISC). To date, this is the first reported case of FcaPV-5 infection in a cat in Japan, and the second case reported worldwide. For the first time this papillomavirus type is associated with BISC development.

KEY WORDS: Bowenoid *in situ* carcinoma, cat, feline papillomavirus, viral plaque

J. Vet. Med. Sci.

81(5): 660–666, 2019

doi: 10.1292/jvms.18-0771

Received: 26 December 2018

Accepted: 11 March 2019

Published online in J-STAGE:
21 March 2019

Papillomavirus is a non-enveloped, circular double-stranded DNA virus, known to infect epidermal and mucosal cells [24]. In general, papillomaviruses are species-specific, and are classified by the DNA sequence similarities of major capsid protein L1 open reading frame (ORF) [24]. Papillomavirus-associated lesions have been uncommonly reported in cats [12, 23]. To date, five *Felis catus* papillomavirus (FcaPV) types have been detected in various lesions, including gingivitis (FcaPV-4), oral papilloma (FcaPV-1), viral plaques (FcaPV-2 and -5), Bowenoid *in situ* carcinoma (BISC) (FcaPV-2 and -3) and cutaneous squamous cell carcinoma (FcaPV-2) [5, 6, 12, 14, 15, 17–20]. In particular, FcaPV-5 is a newly recognized virus type and histological information on its associated lesions has been limited to a single case reported in New Zealand [15, 17]. The present study describes the histopathological, immunohistochemical (IHC), ultrastructural and molecular findings of viral plaques and BISC associated with FcaPV-5 infection in a cat in Japan.

A 17-year-old castrated male Domestic Shorthair cat was presented to a private veterinary clinic with complaint of a mass in the neck region. Clinical examination revealed a solid, crusting dermal mass (1.5 × 1.4 × 0.7 cm) on the left side of the neck. The mass was surgically resected, fixed in 10% phosphate-buffered formalin solution and routinely processed for microscopic examination.

Histological examination revealed multicentric epidermal acanthosis and a well-demarcated tumor lobule confined by the basement membrane (Fig. 1A). The epidermal hyperplasia occasionally involved the follicular infundibulum, where a mild to moderate degree of sebaceous hyperplasia was observed (Fig. 1B). Keratinocytes in the affected epidermis were markedly swollen and had a blue-gray vacuolated cytoplasm. The nucleus of these cells was eccentric, hyperchromatic and sometimes had a shrunken appearance accompanied by perinuclear halo or clear cytoplasm (koilocytes) (Fig. 1B, inset). The thickened epidermis progressed to a tumor lobule with central keratinization, along with marked anisocytosis and anisokaryosis (Fig. 1C). In addition to the aforementioned dysplastic changes, numerous keratinocytes in the tumor lobule contained basophilic, intracytoplasmic inclusion-

*Correspondence to: Chambers, J. K.: achamber@mail.ecc.u-tokyo.ac.jp #These authors contributed equally to this work.

©2019 The Japanese Society of Veterinary Science



This is an open-access article distributed under the terms of the Creative Commons Attribution Non-Commercial No Derivatives (by-nc-nd) License. (CC-BY-NC-ND 4.0: <https://creativecommons.org/licenses/by-nc-nd/4.0/>)

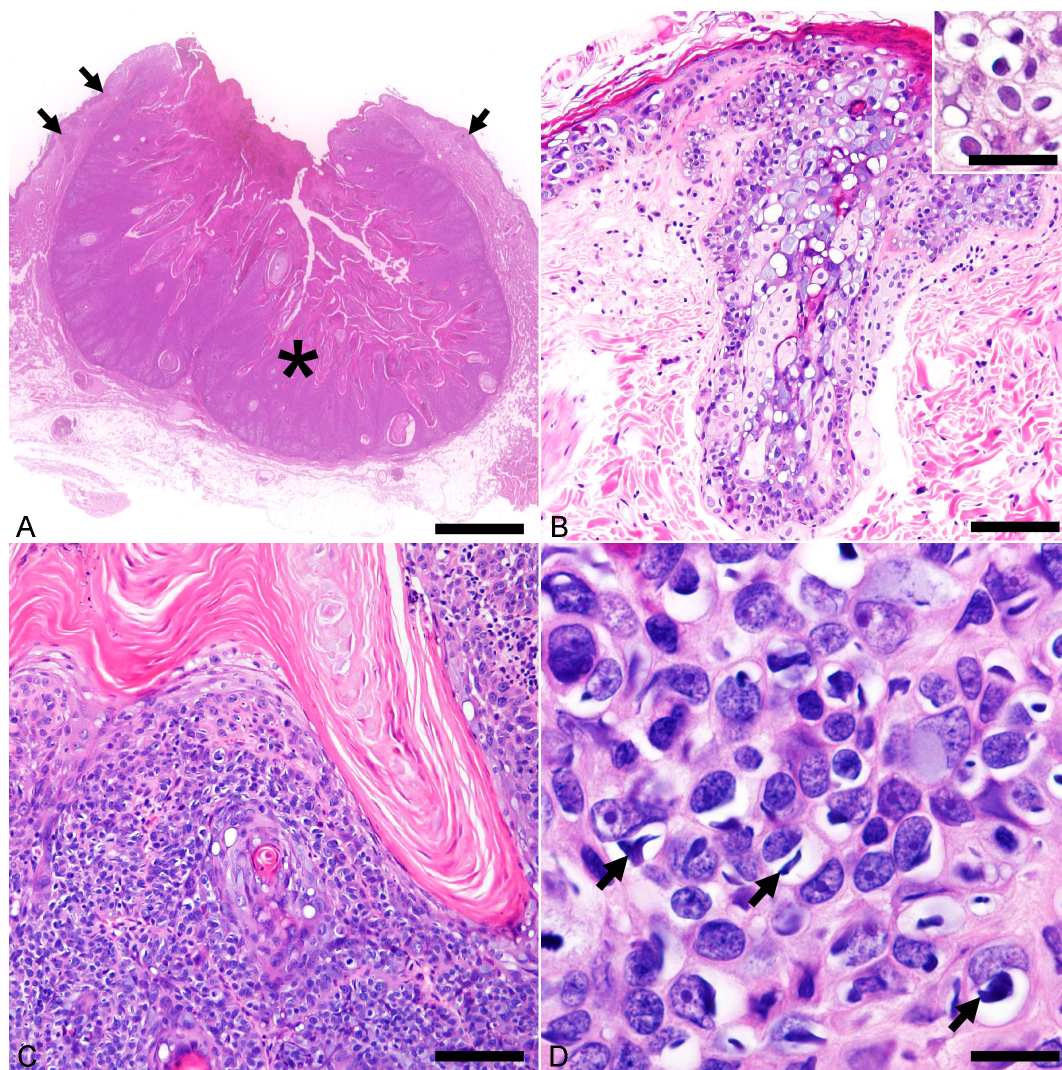


Fig. 1. Histopathological features of *Felis catus* papillomavirus type 5 (FcaPV-5)-associated viral plaque and Bowenoid *in situ* carcinoma (BISC). Hematoxylin and eosin. (A) The neck mass consists of multicentric viral plaques (arrows) and a well-demarcated, keratinizing tumor lobule (asterisk). Bar, 2.5 mm. (B) The viral plaque consists of prominent epidermal and infundibular acanthosis accompanied by mild to moderate sebaceous hyperplasia. The affected suprabasal cells are swollen and have a blue-gray vacuolated cytoplasm. Bar, 100 μ m. Inset shows koilocytes located in the stratum spinosum of acanthotic epidermis. Bar, 40 μ m. (C) Cells of BISC proliferate in nests that are separated by thin fibrous stroma. Bar, 100 μ m. (D) A high magnification shows cells of BISC display marked anisocytosis and anisokaryosis. Numerous cells have a clear swollen cytoplasm with spindle- to irregular-shaped, basophilic cytoplasmic bodies (arrows). Bar, 15 μ m.

like structures (cytoplasmic bodies) (Fig. 1D). Owing to the specific cytopathic changes (i.e. koilocytotic atypia, cytoplasmic basophilia and cytoplasmic bodies), an association between the cutaneous lesions and papillomavirus infection was suspected.

The detection of papillomavirus DNA was performed by polymerase chain reaction (PCR) analysis. Total DNA was extracted from formalin-fixed and paraffin-embedded sections using QIAmp DNA FFPE Tissue Kit (Qiagen, Hilden, Germany) according to the manufacturer's protocol. Sections used for PCR analysis contained both the hyperplastic epidermis and tumor lobule. The success in DNA extraction was confirmed by PCR with feline beta-actin primer pair [8]. A papillomavirus consensus primer pair, MY09/11 was used to detect the L1 ORF of papillomaviral DNA [11]. For detection of FcaPV-5 L1 DNA, a type-specific primer pair, FcaPV-5 L1-1 F/R (5'-ATGGAGGGTGTTCACGTAAG-3'/5'-CATTGGCACCCAGATCTGTC-3') was designed according to the reference sequence of the FcaPV-5 L1 gene, from nucleotide 5,794 to 6,247. Papillomavirus DNA was then amplified using both MY09/11 and FcaPV-5 L1-1 F/R primer pairs. For the MY09/11 primer set, sequencing of the amplicon showed that the amplified DNA sequence had a 100% similarity with the reference FcaPV-5 (GenBank accession number: LC432493, 6,553–6,964 nt, 412 bp, primer region excluded). Sequencing of the amplicon produced by FcaPV-5 L1-1 F/R primer set also revealed a 100% nucleotide similarity with the reference alignment of FcaPV-5 from nucleotide 5,818 to 6,226, in the size of 409 bp, without the primer region (sequence deposited under GenBank accession number LC432492).

Immunohistochemical detection of papillomavirus antigens was carried out using a cocktail of two monoclonal antibodies

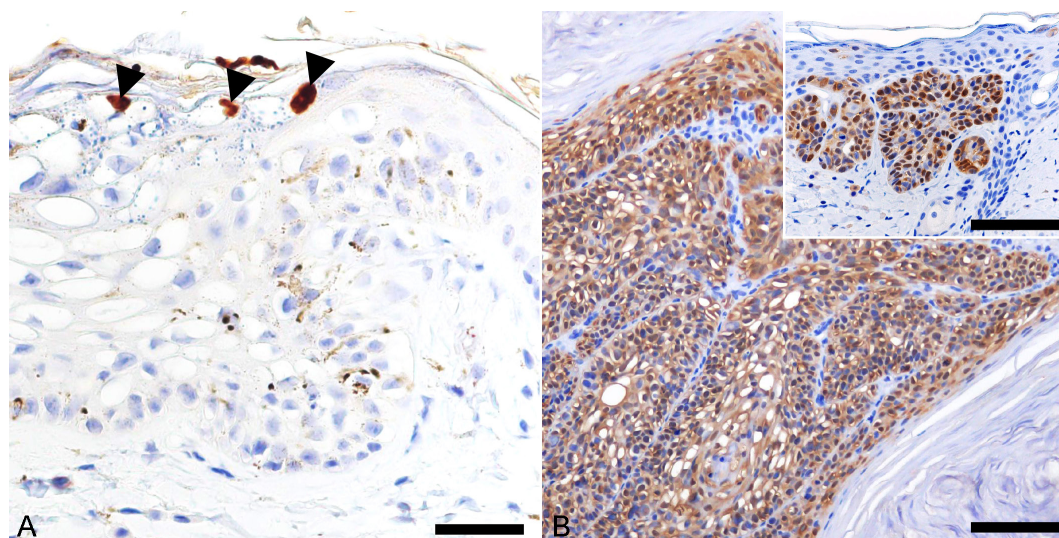


Fig. 2. Immunohistochemical features of viral plaque and Bowenoid *in situ* carcinoma (BISC). Hematoxylin counterstain. (A) Intranuclear localization of papillomaviral antigen in a few koilocytes in the stratum granulosum of the viral plaque. Bar, 30 μm . (B) Cells of BISC display intense nuclear and cytoplasmic immunostaining for p16. Bar, 45 μm . Inset: Strong immunostaining for p16 is observed in the viral plaque. Bar, 100 μm .

(clone BPV-1/1H8 + CAMVIR; Abcam, Cambridge, MA, U.S.A.), which was produced against the major capsid protein of bovine papillomavirus type 1 (BPV-1) and human papillomavirus type 16. The antibody cocktail has been shown to detect a wide range of papillomavirus types in different animal species [1, 10, 25]. Intranuclear localization of papillomaviral antigen was detected in a few koilocytes at the stratum granulosum of the hyperplastic epidermis (Fig. 2A), but not in the tumor lobule.

Based on the histopathological, PCR and IHC findings, the multicentric epidermal acanthosis was classified as viral plaque, while the tumor lobule was diagnosed as Bowenoid *in situ* carcinoma associated with *Felis catus* papillomavirus type 5 infection.

Further IHC analysis was performed to characterize the cutaneous lesions by employing antibodies against cell cycle protein p16 (clone G175-405; BD Pharmingen™, Tokyo, Japan), apoptotic markers, p53 (FL-393; Santa Cruz Biotechnology, Santa Cruz, CA, U.S.A.) and p63 (clone BC4A4, Biocare Medical, Concord, CA, U.S.A.), and cytokeratin (CK) proteins: CK10 (clone DE-K10; Thermo Fisher Scientific, Waltham, MA, U.S.A.), CK14 (clone NCL-L-LL002; Leica Biosystems, MK, U.K.), CK15 (clone LHK15; Thermo Fisher Scientific) and CK19 (clone b170; Leica Biosystems). Both the viral plaque and BISC displayed diffuse nuclear and cytoplasmic immunoreactivity to p16 (Fig. 2B). The p16 protein is a cyclin-dependent kinase (CDK) inhibitor which inactivates CDK4 and CDK6, thereby preventing phosphorylation of retinoblastoma and decelerating the cell cycle [21]. In cats, previous literature has shown that FcpPV-2 and -3 associated viral plaques and BISC displayed an increased immunoreactivity for p16 protein, most probably as a result of retinoblastoma protein inactivation by the papillomavirus oncoproteins [13, 16, 19]. Similarly, intense p16 immunostaining throughout the cutaneous lesions supports a papillomavirus aetiology of the present case.

Intranuclear immunoreactivity for p53 was detected in few basal cells and spinous keratinocytes of the viral plaque (Fig. 3A), but not in the BISC (Fig. 3B). Degradation of p53 protein by oncoprotein has been shown in high-risk human papillomavirus [2]; however, this is not observed in feline papillomaviruses [13]. A plausible explanation for the loss of p53 immunostaining in the BISC is that spontaneous mutations occurred as the lesion progressed. Similar hypothesis has been made in a previous study examining retinoblastoma protein and p53 expression in papillomavirus-associated lesions in cats [13]. Cytokeratin expression profiling was performed to examine cellular phenotype of the viral plaque and BISC, and their corresponding profiles were compared with those of the healthy epidermis and hair follicle in two cats. The cells of viral plaque and BISC displayed increased immunoreactivity for CK14 (Fig. 3C and 3D) and p63. A decreased CK10 immunoreactivity was detected in the stratum granulosum of the viral plaque (Fig. 3E), while the BISC was negative (Fig. 3F). CK14 and p63 are known to be expressed in basal cells and proliferating keratinocytes, while CK10 immunostaining is mainly associated with terminally differentiated keratinocytes [9]. The findings of CK14, p63 and CK10 expressions indicate a proliferative state of the papillomavirus-affected cutaneous lesions. CK15 and CK19 are markers for hair follicle stem cells [9]. In healthy feline skin, CK15 and CK19 were specifically expressed in basal layer of the hair follicle isthmic outer root sheath and suprabulbar region, respectively. In the present case, aberrant CK15 and CK19 immunoreactivities were observed in the basal cells of the viral plaque (Fig. 3G), but not in BISC (Fig. 3H), suggesting a change in epidermal stem cell dynamics during the early course of FcpPV-5 infection.

Transmission electron microscopy was carried out to detect papillomavirus particles and examine the cytopathic changes. Formalin-fixed samples of the skin lesions were washed with phosphate-buffered saline (pH 7.4) and then post-fixed in 1% osmium tetroxide. After that, samples were cut into smaller pieces and embedded in resin Luveak-812 (Nacalai Tesque, Kyoto, Japan). Sections of 1 μm -thick were cut and stained with toluidine blue for preliminary examination under a light microscope. Uranyl acetate and lead nitrate solutions-stained ultrathin sections were then examined with a transmission electron microscope

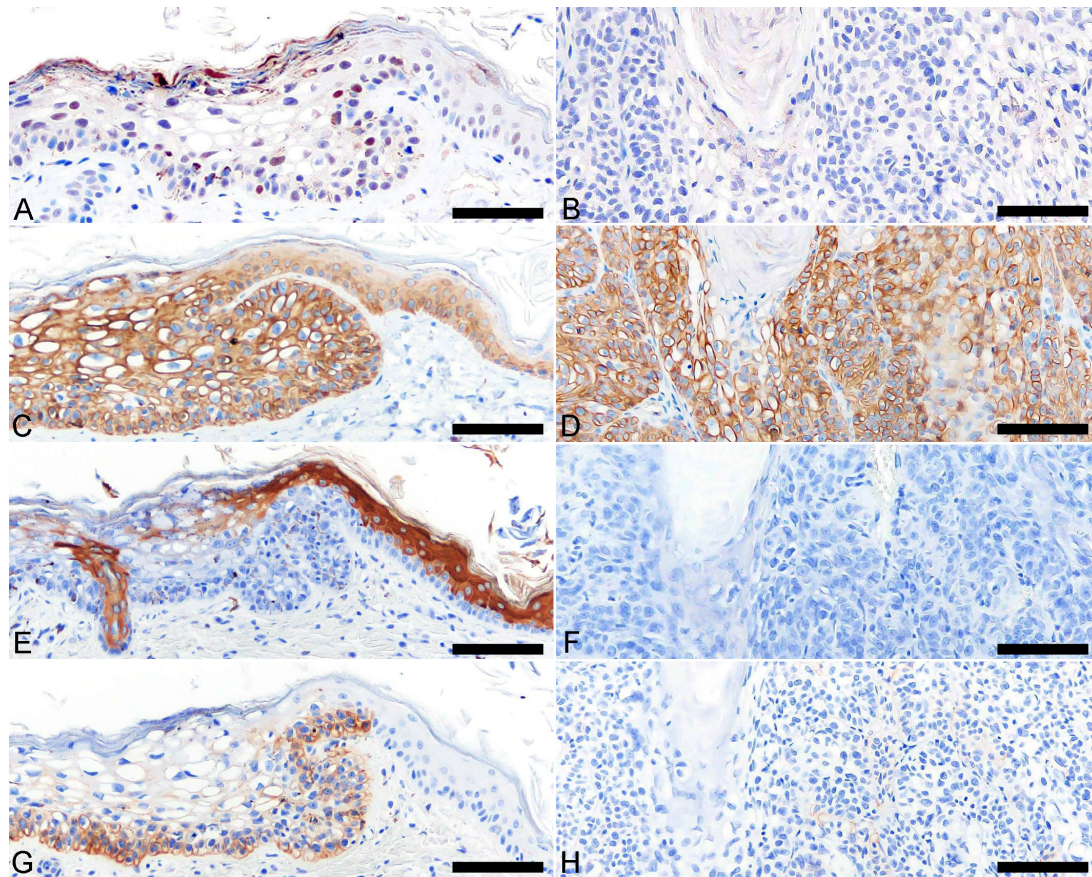


Fig. 3. Immunohistochemical features of viral plaque and Bowenoid *in situ* carcinoma (BISC) (continued). Hematoxylin counterstain. (A) Some keratinocytes of the viral plaque show nuclear immunostaining for p53. (B) Immunoreactivity for p53 is not detected in cells of BISC. (C) Cytokeratin (CK) 14 is diffusely expressed in the viral plaque and (D) BISC. (E) CK10 is weakly positive in the stratum granulosum of the viral plaque; while a strong immunostaining is detected in the hair follicle infundibulum and suprabasal layer of adjacent healthy epidermis. (F) BISC is negative for CK10. (G) CK19 is expressed in the basal cells of the viral plaque and its immunostaining gradually decrease towards the suprabasal layer. The adjacent healthy epidermis is negative for CK19. (H) BISC is negative for CK19. Bar, 60 μ m.

(JEM-1400Plus, JEOL, Tokyo, Japan). No virus particles were detected in all sections examined. This may be due to the relative insensitivity of electron microscopy, as compared with molecular and IHC techniques in detecting the presence of virus in low numbers. Cytoplasmic bodies, frequently detected in cells of BISC with clear cytoplasm, appeared as spindle- to irregular-shaped, electron-dense aggregates (2–13 μ m in diameter) (Fig. 4A and 4B), which shared similar ultrastructural features with keratohyalin granules. On higher magnification, cytoplasmic spaces were entrapped within aggregated amorphous to filamentous materials, thus giving the cytoplasmic body a ‘vacuolated’ appearance (Fig. 4C). Several previous studies have examined the ultrastructural characteristics of papillomavirus-associated cytoplasmic bodies in domestic cats and Asiatic lions (*Panthera leo persica*) [3, 22, 23]. Cytoplasmic bodies in these studies were described as having a granular to fibrillar appearance and were interpreted as aberrant intermediate filament assembly [3, 22, 23]. The cytoplasmic bodies in the present case may be comprised of aggregated keratohyalin and/or intermediate filaments.

In situ hybridization was performed to detect papillomaviral DNA on the tissue sections. Digoxigenin (DIG)-labeled internal DNA probes specific against FcaPV-5 L1 capsid gene, and probes targeting the E6 and E7 oncogene (E6/E7), were synthesized using PCR primer sets: FcaPV-5-L1F 5'- GGATGATAGGCTTAACACTTCTTTAGATCC and FcaPV-5-L1R 5'- AGCCTTAAAATTCATAGCTCCGAATCC, 208 bp; FcaPV-5-E6/E7F 5'- AGGGGTGCTGTCTCCGTTTA and FcaPV5-E6/E7R 5'- CAGCAAGTAAATTGGCGGGC, 316 bp, respectively, which were then labeled with DIG using the DIG DNA Labeling Kit (Roche Diagnostics, Mannheim, Germany) according to the manufacturer’s protocol. After Pronase (room temperature; Biocare Medical) and autoclave pretreatment in citrate buffer, tissue sections were hybridized with one of the Dig-labeled DNA probes. A strong nucleus-associated hybridization signals for L1 (Fig. 5A) and E6/E7 genes were observed in the stratum spinosum of the viral plaque. In the BISC, less than 5% of the cells displayed a positive signal for E6/E7 oncogene (Fig. 5B), while hybridization signal for L1 gene was not detected. The weak hybridization signal within BISC may be attributed to the impairment of viral replication as epidermal dysplasia increases [14]. Papillomavirus E6 and E7 are potential oncogenes which can degrade p53 and inactivate retinoblastoma proteins, respectively, contributing to the proliferation and malignant transformation of infected

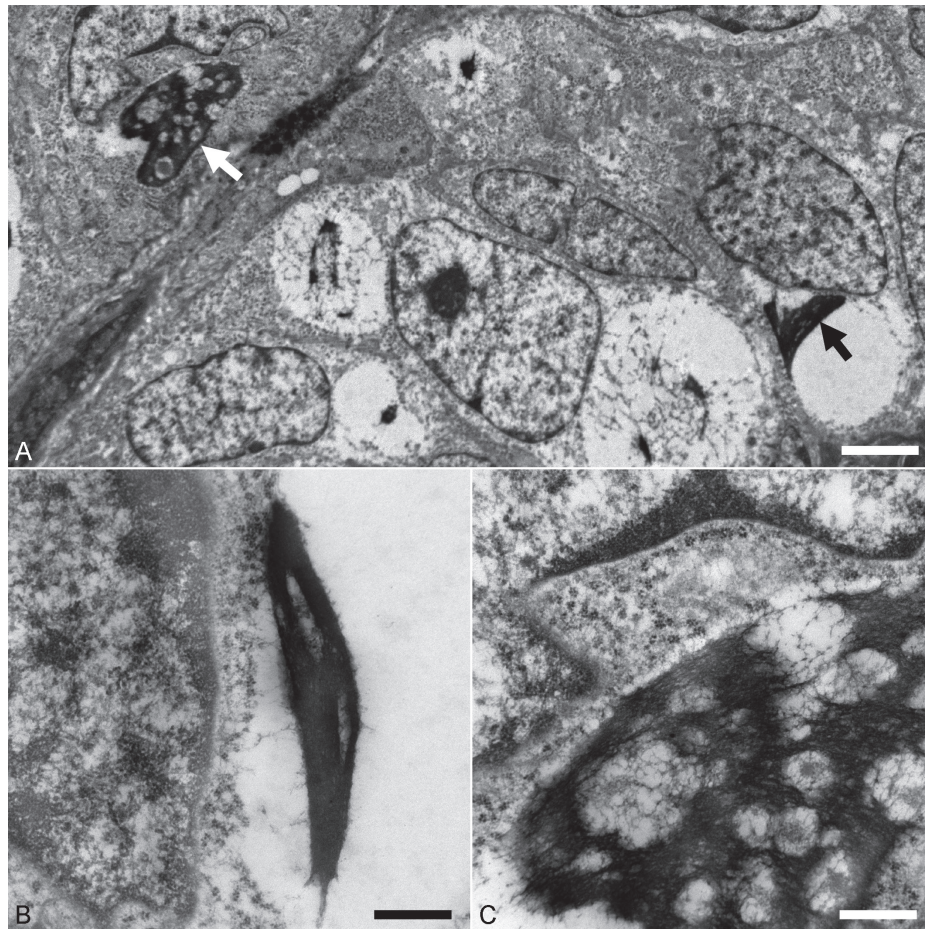


Fig. 4. Transmission electron microscopy showing the ultrastructure of Bowenoid *in situ* carcinoma. (A) Cells contain spindle- to irregular-shaped cytoplasmic bodies (arrows). Bar, 2.4 μm . (B) Cytoplasmic body in a cell consists of spindle-shaped, electron-dense amorphous aggregate. Bar, 0.6 μm . (C) Electron-dense aggregate of amorphous to filamentous materials and entrapped cytoplasmic spaces which give the cytoplasmic body a 'vacuolated' appearance. Bar, 0.6 μm .

keratinocytes [2]. This is particularly true for some types of high-risk alpha human papillomavirus [2, 14]. Similar to FcaPV-2 infection, the FcaPV-5 E7 oncoprotein may have inactivated the retinoblastoma protein, thereby disrupting the p16-retinoblastoma pathway and leading to accumulation of p16 protein [16]. The dysregulation of cell cycle eventually promotes proliferation of the viral plaque. Spontaneous mutations of p53, which occur independent of E6 oncogene, may have facilitated the progression of viral plaque to BISC [13].

Felis catus papillomavirus type-5 is a recently discovered papillomavirus, first isolated from the viral plaque lesions of a cat in New Zealand in 2017 [15, 17]. Due to its low reported incidence, the epidemiology and pathogenicity of FcaPV-5 are still poorly understood. The current detection of FcaPV-5 in Japan indicates a wide geographical distribution of this FcaPV type. In the present case, feline viral plaque was histologically characterized by epidermal and infundibular acanthosis with sebaceous hyperplasia. Proliferation of sebaceous glands was observed in areas with infundibular acanthosis, while the hyperplastic epidermis and BISC were devoid of sebaceous component. This suggests that sebaceous hyperplasia occurred following FcaPV-5 infection of the upper hair follicle segment and support the hypothesis that FcaPV-5 is able to infect a wider range of cutaneous epithelial cell types than other FcaPV types. Basal cell carcinoma was considered as a differential diagnosis for the tumor lobule, but was ruled out based on the presence of intact basement membrane and absence of infiltrative growth pattern. Expansive growth into the deeper dermis, and marked anisocytosis and anisokaryosis exhibited by the tumor lobule, likely indicates an advanced BISC lesion [7].

The FcaPV-5-associated lesions exhibited several cytopathic changes, including nuclear shrinkage, perinuclear halo, blue-gray vacuolated cytoplasm and cytoplasmic bodies. In particular, cytoplasmic bodies detected in BISC have not been reported in lesions caused by FcaPV-2. A recent study have observed similar intracytoplasmic inclusions in FcaPV-3 associated basal cell carcinoma and BISCs [19]. FcaPV-5 is closely associated with FcaPV-3, as depicted by their ORF L1 similarity, and the described cytoplasmic bodies may represent a unique histological feature of this novel papillomavirus genus. In humans, cytoplasmic bodies are observed in cutaneous lesions caused by a subset of papillomavirus types. In particular, Beta, Gamma and MU Human Papillomaviruses infected keratinocytes displayed prominent cytoplasmic bodies that are composed mainly of E4 protein [4]. Intracytoplasmic assembly of E4 protein has been thought to support the viral genome amplification [4]. The significance of cytoplasmic bodies

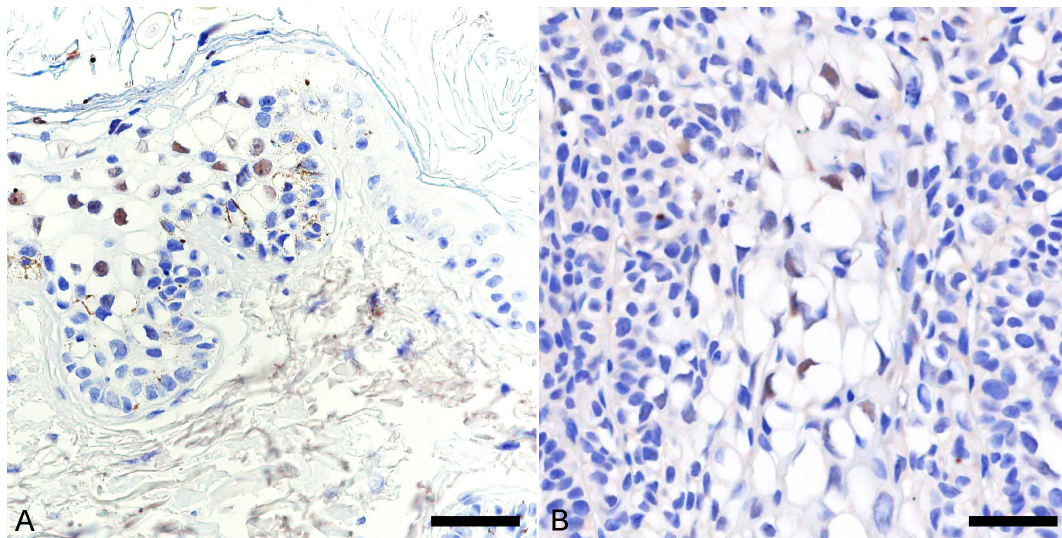


Fig. 5. (A) Strong nucleus-associated hybridization signals for L1 gene are observed in stratum spinosum of the viral plaque. *In situ* hybridization. Hematoxylin counterstain. Bar, 40 μ m. (B) In Bowenoid *in situ* carcinoma, less than 5% of the cells display a positive signal for E6/E7 gene. *In situ* hybridization. Hematoxylin counterstain. Bar, 30 μ m.

in the pathogenesis of FcaPV-3 and -5 remains unclear, although they are considered as a cytopathic change associated with productive papillomavirus infections [23].

In summary, the present case report describes FcaPV-5-associated viral plaques and BISC in a geriatric cat. To date, this is the first reported case of FcaPV-5 infection in a cat in Japan, and the second case reported worldwide. For the first time, we found that FcaPV-5 is associated with BISC development, and keratinocytes within the lesion contained basophilic cytoplasmic bodies not observed in FcaPV-2 associated BISC.

CONFLICT OF INTERESTS. The author(s) declared no potential conflicts of interest with respect to the research, authorship, and/or publication of this article.

FUNDING. The authors received no financial support for the research, authorship, and/or publication of this article.

ACKNOWLEDGMENT. The authors are grateful to Ms. S. Kato for her invaluable technical assistance.

REFERENCES

1. Beckwith-Cohen, B., Teixeira, L. B., Ramos-Vara, J. A. and Dubielzig, R. R. 2015. Squamous papillomas of the conjunctiva in dogs: a condition not associated with papillomavirus infection. *Vet. Pathol.* **52**: 676–680. [Medline] [CrossRef]
2. Boulet, G., Horvath, C., Vanden Broeck, D., Sahebali, S. and Bogers, J. 2007. Human papillomavirus: E6 and E7 oncogenes. *Int. J. Biochem. Cell Biol.* **39**: 2006–2011. [Medline] [CrossRef]
3. Carney, H. C., England, J. J., Hodgins, E. C., Whiteley, H. E., Adkison, D. L. and Sundberg, J. P. 1990. Papillomavirus infection of aged Persian cats. *J. Vet. Diagn. Invest.* **2**: 294–299. [Medline] [CrossRef]
4. Doorbar, J. 2013. The E4 protein; structure, function and patterns of expression. *Virology* **445**: 80–98. [Medline] [CrossRef]
5. Dunowska, M., Munday, J. S., Laurie, R. E. and Hills, S. F. 2014. Genomic characterisation of *Felis catus* papillomavirus 4, a novel papillomavirus detected in the oral cavity of a domestic cat. *Virus Genes* **48**: 111–119. [Medline] [CrossRef]
6. Gil da Costa, R. M., Peleteiro, M. C., Pires, M. A. and DiMaio, D. 2017. An update on canine, feline and bovine papillomaviruses. *Transbound. Emerg. Dis.* **64**: 1371–1379. [Medline] [CrossRef]
7. Goldschmidt, M. H., Munday, J. S., Scruggs, J. L., Klopffleisch, R. and Kiupel, M. 2018. Classification of epithelial tumors of the skin. pp. 38–52. *In: Surgical Pathology of Tumors of Domestic Animals: Volume 1: Epithelial Tumors of the Skin* (Kiupel, M. ed.), Davis-Thompson DVM Foundation, Gurnee.
8. Kessler, Y., Helfer-Hungerbuehler, A. K., Cattori, V., Meli, M. L., Zellweger, B., Ossent, P., Riond, B., Reusch, C. E., Lutz, H. and Hofmann-Lehmann, R. 2009. Quantitative TaqMan real-time PCR assays for gene expression normalisation in feline tissues. *BMC Mol. Biol.* **10**: 106. [Medline] [CrossRef]
9. Kok, M. K., Chambers, J. K., Ong, S. M., Nakayama, H. and Uchida, K. 2018. Hierarchical cluster analysis of cytokeratins and stem cell expression profiles of canine cutaneous epithelial tumors. *Vet. Pathol.* **55**: 821–837. [Medline] [CrossRef]
10. Linder, K. E., Bizikova, P., Luff, J., Zhou, D., Yuan, H., Breuhaus, B., Nelson, E. and Mackay, R. 2018. Generalized papillomatosis in three horses associated with a novel equine papillomavirus (EcPV8). *Vet. Dermatol.* **29**: 72–e30. [Medline] [CrossRef]
11. Manos, M. M., Ting, Y., Wright, D. K., Lewis, J., Broker, T. R. and Wolinsky, S. M. 1989. The use of polymerase chain reaction amplification for

- the detection of genital human papillomaviruses. *Cancer Cells* **7**: 209–214.
12. Munday, J. S. 2014. Papillomaviruses in felids. *Vet. J.* **199**: 340–347. [[Medline](#)] [[CrossRef](#)]
 13. Munday, J. S. and Aberdein, D. 2012. Loss of retinoblastoma protein, but not p53, is associated with the presence of papillomaviral DNA in feline viral plaques, Bowenoid *in situ* carcinomas, and squamous cell carcinomas. *Vet. Pathol.* **49**: 538–545. [[Medline](#)] [[CrossRef](#)]
 14. Munday, J. S. and Kiupel, M. 2010. Papillomavirus-associated cutaneous neoplasia in mammals. *Vet. Pathol.* **47**: 254–264. [[Medline](#)] [[CrossRef](#)]
 15. Munday, J. S., Dittmer, K. E., Thomson, N. A., Hills, S. F. and Laurie, R. E. 2017. Genomic characterisation of *Felis catus* papillomavirus type 5 with proposed classification within a new papillomavirus genus. *Vet. Microbiol.* **207**: 50–55. [[Medline](#)] [[CrossRef](#)]
 16. Munday, J. S., French, A. F., Peters-Kennedy, J., Orbell, G. M. and Gwynne, K. 2011. Increased p16^{CDKN2A} protein within feline cutaneous viral plaques, bowenoid *in situ* carcinomas, and a subset of invasive squamous cell carcinomas. *Vet. Pathol.* **48**: 460–465. [[Medline](#)] [[CrossRef](#)]
 17. Munday, J. S., Marshall, S., Thomson, N. A., Kiupel, M., Heathcott, R. W. and French, A. 2017. Multiple viral plaques with sebaceous differentiation associated with an unclassified papillomavirus type in a cat. *N. Z. Vet. J.* **65**: 219–223. [[Medline](#)] [[CrossRef](#)]
 18. Munday, J. S., Sharp, C. R. and Beatty, J. A. 2019. Novel viruses: update on the significance of papillomavirus infections in cats. *J. Feline Med. Surg.* (in press). [[Medline](#)]
 19. Munday, J. S., Thomson, N. A., Henderson, G., Fairley, R. and Orbell, G. M. 2018. Identification of *Felis catus* papillomavirus 3 in skin neoplasms from four cats. *J. Vet. Diagn. Invest.* **30**: 324–328. [[Medline](#)] [[CrossRef](#)]
 20. Munday, J. S., Thomson, N. A. and Luff, J. A. 2017. Papillomaviruses in dogs and cats. *Vet. J.* **225**: 23–31. [[Medline](#)] [[CrossRef](#)]
 21. Ohtani, N., Yamakoshi, K., Takahashi, A. and Hara, E. 2004. The p16^{INK4a}-RB pathway: molecular link between cellular senescence and tumor suppression. *J. Med. Invest.* **51**: 146–153. [[Medline](#)] [[CrossRef](#)]
 22. Sundberg, J. P., Montali, R. J., Bush, M., Phillips, L. G. Jr., O'Brien, S. J., Jenson, A. B., Burk, R. D. and Van Ranst, M. 1996. Papillomavirus-associated focal oral hyperplasia in wild and captive Asian lions (*Panthera leo persica*). *J. Zoo Wildl. Med.* **27**: 61–70.
 23. Sundberg, J. P., Van Ranst, M., Montali, R., Homer, B. L., Miller, W. H., Rowland, P. H., Scott, D. W., England, J. J., Dunstan, R. W., Mikaelian, I. and Jenson, A. B. 2000. Feline papillomas and papillomaviruses. *Vet. Pathol.* **37**: 1–10. [[Medline](#)] [[CrossRef](#)]
 24. Van Doorslaer, K., Chen, Z., Bernard, H. U., Chan, P. K. S., DeSalle, R., Dillner, J., Forslund, O., Haga, T., McBride, A. A., Villa, L. L., Burk R. D. and Ictv Report Consortium. 2018. ICTV virus taxonomy profile: Papillomaviridae. *J. Gen. Virol.* **99**: 989–990. [[Medline](#)] [[CrossRef](#)]
 25. Yamashita-Kawanishi, N., Sawanobori, R., Matsumiya, K., Uema, A., Chambers, J. K., Uchida, K., Shimakura, H., Tsuzuki, M., Chang, C. Y., Chang, H. W. and Haga, T. 2018. Detection of *felis catus* papillomavirus type 3 and 4 DNA from squamous cell carcinoma cases of cats in Japan. *J. Vet. Med. Sci.* **80**: 1236–1240. [[Medline](#)] [[CrossRef](#)]